JOURNAL OF CATALYSIS **179,** 548–559 (1998)
ARTICLE NO. CA982240

The Dynamic Restructuring of Electrolytic Silver during the Formaldehyde Synthesis Reaction

A. Nagy, G. Mestl, T. Rühle, G. Weinberg, and R. Schlögl

Fritz-Haber-Institut der Max-Planck Gesellschaft, Faradayweg 4-6, D-14195 Berlin, Germany

Received March 3, 1998; revised June 18, 1998; accepted July 19, 1998

The partial oxidation of methanol to formaldehyde was studied over an industrial electrolytic silver catalyst. Special attention was paid to the influence of reaction-induced restructuring of the silver surface and bulk on the activity for the partial oxidation of methanol to formaldehyde. Drastic differences are observed in the performance exhibited by fresh samples and those which have been previously treated at high temperature ($T > 873$ K) reaction conditions. The temperature dependence of the conversion for a fresh catalyst shows a pronounced hysteresis which can be separated into three temperature regimes. These regimes are strongly correlated with various morphological changes induced in the silver during reaction. SEM images reveal that heating silver in an excess of methanol to 773 K results in the destruction of grain-boundary defects. Comparison of the various hysteresis profiles with TDS analysis of silver pretreated at high temperature in oxygen shows that elimination of these defects results in the inhibition of oxygen diffusion from the bulk to the surface in the temperature region between 673 K and 873 K. The formation of holes resulting from the reaction of bulk-dissolved hydrogen and oxygen indicates that diffusion along these defect structures supplies bulk oxygen for the catalytic reaction. Hole formation above 923 K is no longer restricted to grain boundaries, indicating that volume (interstitialcy) diffusion replaces grain-boundary diffusion at elevated temperatures. This incorporation of oxygen into the silver lattice results in an increased conversion of methanol with a higher conversion to formaldehyde. Consequently, no hysteresis is observed subsequent to having treated the sample in the reaction mixture at temperatures in excess of 873 K. Reaction-induced restructuring of the catalyst on the time scale of a typical run occurs. This leads to an improvement in the catalytic performance of silver for this extremely structure-sensitive reaction. © 1998 Academic Press

Key Words: **silver; formaldehyde; methanol; oxidation; diffusion; defect structure; hysteresis; kinetics.**

1. INTRODUCTION

The remarkable catalytic properties of silver have been known for over a hundred years (1). The partial oxidation of methanol to formaldehyde is conducted at significantly higher temperatures (in excess of 800 K) over unsupported, electrolytically prepared silver (1–3). The partial oxidation of ethylene to ethylene oxide is conducted over alumina-supported silver (4,5). This reaction is carried out, industrially, at temperatures lower than 600 K. These extreme differences in temperature, particle size, and catalyst type show the extreme versatility of silver as a partial oxidation catalyst but hint that the mechanisms involved differ significantly. These mechanistic differences arise, in part, from the fact that silver is capable of accommodating a variety of catalytically active oxygen species (6–8). The formation of these species is a complex function of temperature, partial pressure of oxygen, type of silver and is closely related to its pretreatment history (6). Morphological changes occurring at higher temperatures at the silver surface, as well as in the bulk may inhibit or promote the formation of these species. Table 1 shows a summary of these species, as well as a number of others cited in the literature. The three species which are dealt with in this paper are termed O_α, O_β, and O_γ. The former is assigned to chemisorbed, surface-bound atomic oxygen. O_β is bulk-dissolved oxygen which diffuses through high-indexed crystalline structures and along grain boundaries (6). O_γ is the intermediate state where O_β segregates from the bulk to the surface (6–11). It is a strongly bound oxygen species intercalated in the uppermost silver layers (6–11). These species have been extensively studied with a variety of spectroscopic techniques (3,6–14). In these studies, it was found that O_α catalyzes the oxi-dehydrogenation of CH_3OH to formaldehyde. It is a strong nucleophile and therefore tends to react to the complete oxidation reaction products CO_2 and water. O_γ, on the other hand, is believed to only catalyze the selective dehydrogenation of methanol to formaldehyde. It is strongly intercalated ($T_{\mathrm{des}} > 873$ K) in the silver crystal structure and does not form complete oxidation products. This explains the maximum in conversion obtained for the industrial process which is *understoichiometric* in oxygen (1,2) and occurs at temperatures in excess of 873 K, where O_γ is the only stable oxygen species. O_β cannot participate directly in reaction as it is located in the bulk.

The goal of this work is to show that restructuring of silver resulting from the gas–solid interaction leads to the activation of silver for the partial oxidation of methanol to formaldehyde. It is shown that silver plays a dynamic role in

0021-9517/98 $25.00

TABLE 1

Literature Assignments of Various Oxygen Species Adsorbed on Silver Surfaces

Species	Desorption temperature (K)	Location	Assignment	Reference
O_2	25	Surface	Physisorbed	29
O_2	190–300	Surface	Chemisorbed	2,26,30,31,32
O	570–620	Surface	Atomic adsorbed	15,25,26,27,28
O	1120	Subsurface	Strongly bound	14
O	820	Near defects	Species V	4,9,25
O	780–880	Bulk-dissolved	—	13,25,26,30,35
O	580	Surface	Ionic	8
O	740–860	Surface-embedded	Covalent	8,36
O	900	—	Very high T	35
O	619	Subsurface	—	27
O	580	Surface	β	26
O	<600	Surface	α	19,31,37
O	600–900	Bulk-dissolved	β	19,31,37
O	<900	Surface-embedded	γ	19,37

the reaction, adapting to its thermal and chemical environment on the *time scale* of the experiments performed here.

2. EXPERIMENTAL

Electrolytic silver (BASF-AG), silver powder (Chempur 99.9%) and silver foil (Goodfellow 99.9995%) were tested. Qualitative analysis by EDX showed the presence of small amounts of C, Si, and Cl contamination in all samples. The silver foil was polished with diamond paste and used for the SEM experiments. Catalytic experiments were carried out in two different tubular quartz reactors. Both reactors were approximately 20 cm long. The first had an inner diameter of 4 mm and the second, 8 mm. Samples were held in place with quartz-wool plugs. A thermocouple (type K) was attached to the outer wall of the quartz tube directly adjacent to the sample with stainless steel wire. The wall thickness was 1 mm. The high catalytic activity of the thermocouple makes direct placement in the catalyst bed impossible. Quartz chips were used to dilute certain samples in order to differentiate when local heating effects played a significant role. Heating was provided by a single-zone oven (ID = 15 mm) with an isothermal section approximately 1 cm long which was controlled by a Eurotherm temperature controller (model 902). Catalyst particle sizes tested were 0.2–0.4 mm, 0.75–1 mm, and 20 μm. Space velocities varied from 22,000 h^{-1} to 6.7×10^5 h^{-1}. The total flow was kept constant at 265 ml/min and the space velocity was varied by changing the bed height. Linear velocity was therefore 8.8cm/s for runs made with the 4-mm ID reactor and 2.2 cm/s for the 8-mm ID reactor. Pressure drops across the catalyst bed were less than the maximum sensitivity of 0.1 bar. The ratio (ml/min CH_3OH)/(ml/min O_2) of 2.5 is slightly higher than 2.0 which is that used in the industrial process (1). The methanol-rich conditions were chosen in order to minimize local heating effects resulting from the high exothermicity of the complete oxidation reaction which is known to be favored at higher oxygen partial pressures (1,7,14). The following definitions are used throughout this paper:

- %conversion = mol(product)/mol(MeOH in feed) × 100%;
- %selectivity = mol(product)/(mol(MeOH in feed) − mol(MeOH out)) × 100%.

Complete conversion of oxygen occurs for restructured samples having undergone reaction at temperatures higher than 873 K. This makes determination of the intrinsic reaction rate on a per active site basis impossible. For this reason, all data is shown as %conversion. Variation of the dead volume downstream of the catalyst bed resulted in a change in activity indicating the presence of gas-phase, homogeneously catalyzed reactions. This could not be studied in detail, as a large temperature gradient exists over the length of the entire oven making a quantitative determination of the role of gas-phase reactions impossible. The empty reactor shows no activity. Analysis of the products was made by on-line gas chromatography. A mol-sieve (5A) (Supelco) and a carboxen (Supelco) column were used for separation of both high and low boiling point compounds. Quantitative analysis of all compounds except water was possible with this setup. Heating rates of 0.5 K/min and 1 K/min, combined with a sampling time of 30 min results in a temperature resolution of 15 K and 30 K, respectively. It is assumed that the values obtained for these extremely slow heating rates are representative of the steady-state values. This is confirmed by the fact that the activation energies and conversions calculated using the different heating rates (1 K/min) and (0.5 K/min) are identical within an acceptable margin of error.

TDS measurements were made in an UHV chamber with an average background pressure of 3×10^{-8} mbar (background gas is primarily H_2O). Monitoring of desorption products was made with a Hiden (Hal2) quadrupole mass spectrometer coupled to a Next workstation. A sampling rate of 1 s was standard. A homemade convection oven was used for heating. The thermocouple (type K) was placed immediately below the sample and was in direct contact with the quartz holding tube. Linear heating rates from room temperature to 1000 K were possible with this setup. A heating rate of 1 K/s was used for all TDS runs. A special pretreatment procedure was used in order to minimize the amount of carbon present in the sample. This consisted of treating the sample in flowing O_2 (17 ml/min) at 973 K, transferring to the UHV through air and subsequently performing numerous oxidation–reduction cycles. This had to be done for approximately one week before a sufficiently clean sample was obtained.

The SEM images were taken with a Hitachi S-4000 SEM equipped with an EDX for element identification.

3. RESULTS

3.1. The Conversion Obtained over an Aged Catalyst

Reproducible results were obtained after repeating three high-temperature reaction ($T > 923$ K) cycles with subsequent cooling in the reaction mixture. No deactivation was observed for samples subjected to this pretreatment. A typical run made with a used silver catalyst is shown in Fig. 1. The light-off temperature is approximately 500 K. The exothermicity of the prevailing net-oxidation reaction results in a temperature rise of approximately 50 K. A measurement with N_2 instead of He as the carrier gas ($5 \times$ reduction in heat conductivity) showed the same conversion. This is evidence that local-heating of the catalyst bed is not responsible for CO_2 formation in this temperature range. The formation of complete oxidation products is attributed to the reaction of methanol with the weakly bound atomic surface oxygen species O_α. Above 500 K, CO_2 yield drops off and the formaldehyde yield increases. Oxygen is completely consumed above 500 K (Fig. 1). The complete conversion of oxygen implies that only a portion of the catalyst bed is being used for reaction. This is also the case for beds which are only 1-mm thick. Incomplete oxygen conversion above 573 K is only obtained for samples containing an extremely small amount of silver thinned with quartz (0.06 g Ag : 0.24 g, SiO_2 : 0.4–0.7 mm : 0.2–0.4 mm) or for fresh samples which have not undergone previous high-temperature reaction. Channeling of reactants through the thinned bed is likely under these conditions and the results are therefore not shown here. The complete consumption of oxygen makes it impossible to conduct a kinetic analysis of the methanol oxidation reaction with this reactor setup. The methanol conversion rises with increasing conversion

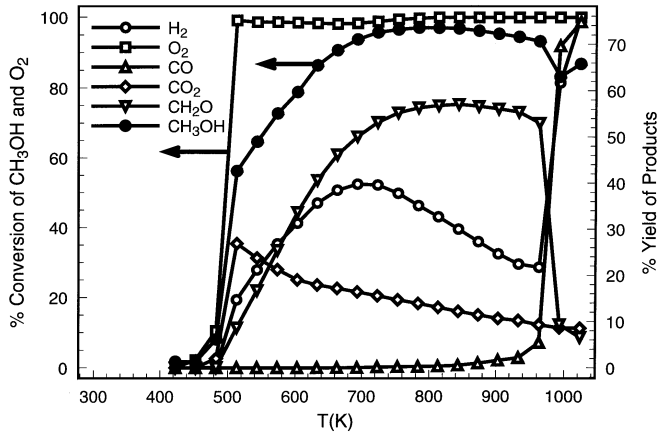

FIG. 1. Percentage conversion of methanol to selected products over an aged electrolytic silver catalyst. Heating rate 1 K/min, 0.3 g Ag (0.75–1 mm), 3.5 vol% O_2, 8.8 vol% CH_3OH, 87.7 vol% He, S.V. $= 3.63 \times 10^5\ h^{-1}$.

to formaldehyde and levels off at about 773 K. The abrupt drop in formaldehyde production and subsequent formation of H_2 and CO at 973 K is due to the gas-phase decomposition of methanol and formaldehyde. This represents the upper-temperature limit for all experiments presented here.

3.2. The Conversion Obtained with a Fresh Catalyst

Figure 2 shows the first run obtained using the fresh catalyst charge which was subsequently used to produce Fig. 1. The light-off temperature of the fresh catalyst is approximately 80 K higher than that of the aged one. The fresh catalyst initially behaves in the same fashion as the aged catalyst but shows a strong deactivation with heating above 573 K. The deactivation leads to a minimum in methanol conversion (13%) at approximately 850 K. Above this temperature, the conversion rises sharply. The gas-phase mixture decomposes homogeneously (see Section 3.1.2) above 973 K producing primarily CO and H_2. The deactivation results in a minimum in conversion at 800 K after which the CH_3OH and O_2 conversion increases sharply (approximately 850 K).

3.3. The Hysteresis of Reaction

3.3.1. Cycle 1 (423–573–423 K). Hysteresis experiments were performed in order to provide more information about the cause of the deactivation. The presence of hysteresis indicates either a temperature bistability of the system or an intrinsic change of the catalyst activity such as the creation and/or destruction of active sites. The chosen end-temperatures for the hysteresis experiments correspond to the first maximum in methanol conversion at 573 K, the minimum at 773 K and the second maximum in conversion at 873 K in Fig. 2. Runs were made with heating and cooling ramps of either 1 K/min or 0.5 K/min. The 0.5 K/min run was diluted with quartz chips. Comparison of these runs allows

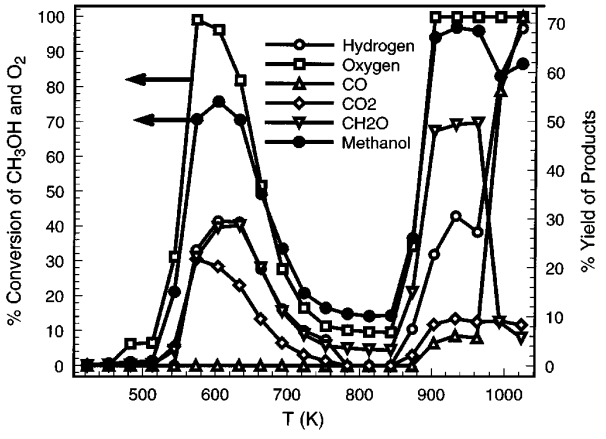

FIG. 2. Percentage conversion to selected products over a fresh electrolytic silver catalyst, heating rate 1 K/min, 0.3 g fresh Ag (0.75–1.0 mm), 3.5 vol% O_2, 8.8 vol% CH_3OH, 87.7 vol% He, S.V. $= 3.63 \times 10^5$ h^{-1}.

the differentiation between hysteresis effects caused by local heating and those which are due to intrinsic changes in the catalyst sample. The results are shown in Figs. 3–5. Figure 3 shows the methanol-conversion hysteresis obtained for the cycle 423 K–573 K–423 K using the two different heating rates of 0.5 K/min and 1 K/min, with and without thinning with quartz chips. This plot reveals that the hysteresis observed in this temperature range is likely an artifact. The reaction is highly exothermic in this temperature range due to the highly oxidative nature of the O_α oxygen species formed on the silver surface (3,12,14,26). The heating portion of the cycle in Fig. 3 is likely to be more representative of the true temperature-conversion profile than the cooling branch.

3.3.2. Cycle 2 (423–773–423 K). Figures 4a and 4b show the hysteresis plots obtained for methanol conversion and formaldehyde yield in the temperature region (423–773–423 K//0.5 K/min). The maximum temperature for this cycle coincides with the observed minimum in activity shown in Fig. 2. The conversion for both species passes through a maximum at 660 K and then decreases with increasing temperature. The decrease in activity when approaching 773 K is not immediately reversed upon cooling. Rather, the sample appears to be progressively deactivated with cooling until approximately 673 K.

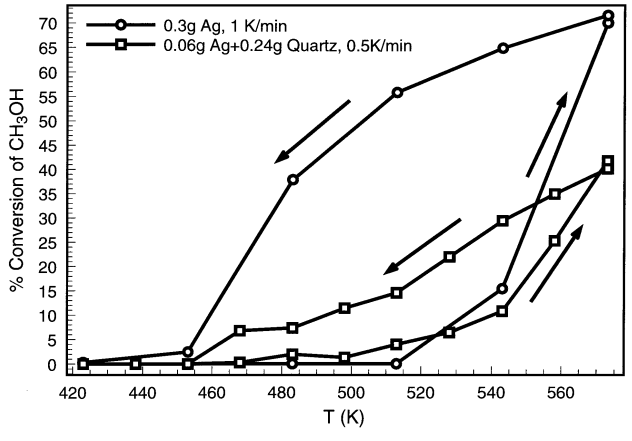

FIG. 3. Comparison of hysteresis profiles for samples with and without thinning by quartz chips at two different heating rates (0.75–1.0 mm), 3.5 vol% O_2, 8.8 vol% CH_3OH, 87.7 vol% He, S.V. $= 1.68 \times 10^5$ h^{-1}.

3.3.3. Cycle 3 (423–948–423 K). Figures 5a and 5b show the hysteresis plots obtained for methanol conversion and formaldehyde yield for cycle 3 (423–948–423 K//0.5 K/min). A deactivation of the catalyst similar to that observed for the ascending temperature branch in cycle 2 (Figs. 4a and 4b) is also seen for the ascending branch here. The first small maximum in methanol conversion obtained at 623 K for this cycle is, however, approximately 30% lower than that shown in cycle 1 (Fig. 3). The deactivation observed for the ascending branch from 423 K to 948 K (see Figs. 5a and 5b) is not observed for the descending branch. The high-temperature treatment has irreversibly modified the catalyst. Subsequent runs made with this catalyst showed no hysteresis and exhibit temperature-conversion plots whose form is identical to that seen in Fig. 1.

3.4. Arrhenius Plot for Used Silver

Figure 6 shows the Arrhenius plot for a silver catalyst after having undergone three reaction cycles (max temp = 1023 K, 1 K/min). This plot is based on methanol conversion and not on the actual rate of reaction. Only the activation energies should, therefore, be representative of the *apparent* activation energies as determination of the frequency factor requires the intrinsic reaction rate to be known. Determination of the intrinsic rate is made impossible by the very high conversions obtained. The extremely small activation energies indicate that the reaction, as performed under these conditions, is diffusion limited. Variation of the activation energy signifies a change of mechanism or the presence of diffusion inhibition. Two inflection points are seen in Fig. 6. These points separate the Arrhenius curve into a number of linear segments which are indicated by vertical lines.

3.5. Temperature Desorption Spectroscopy (TDS) of O_2 on Electrolytic Silver

Figure 7 shows a typical TD spectrum for a sample dosed with 300 mbar O_2 at 973 K. Two peaks are clearly visible. The first is a broad, asymmetric peak centered at 936 K with a high-temperature tail and is assigned to O_β. The second is not baseline-resolved, begins at approximately 923 K, and is assigned to O_γ. The pretreatment was made above the thermal-desorption temperature of O_α (573 K). It is therefore not present in the spectra.

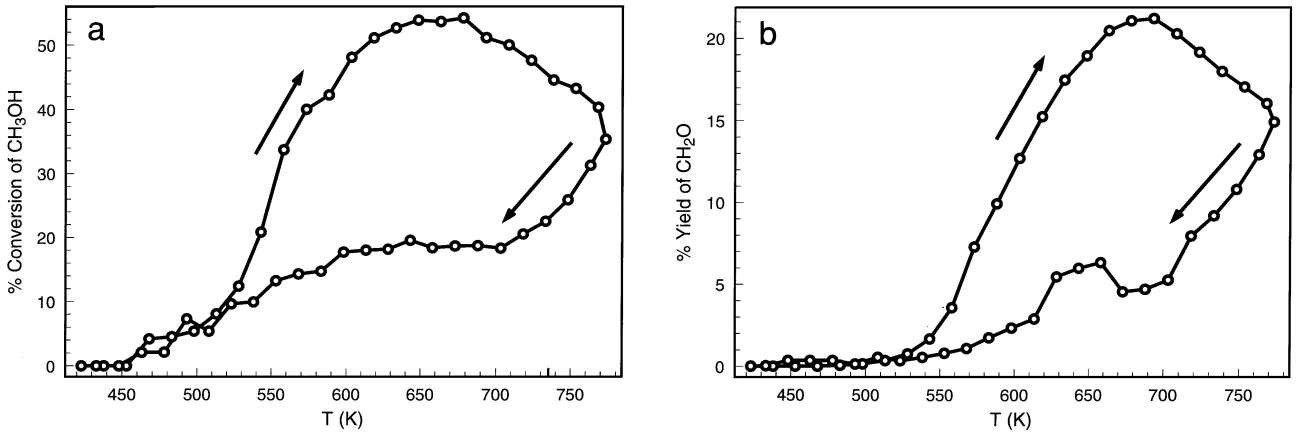

FIG. 4. (a) Percentage conversion of CH_3OH for the cycle (423–773–423 K), 0.5 K/min, 0.06 g Ag + 0.06 g quartz, 4.3 vol% O_2, 7.1 vol% CH_3OH, 88.6 vol% He, S.V. = 1.68×10^5 h^{-1}. (b) Percentage CH_2O yield for the cycle (423–773–423 K), 0.5 K/min, 0.06 g Ag + 0.06 g quartz, 4.3 vol% O_2, 7.1 vol% CH_3OH, 88.6 vol% He, S.V. = 1.68×10^5 h^{-1}.

3.6. Scanning Electron Microscopy Analysis of the Treated Ag Foil

SEM images of the fresh sample, as well as those subsequent to treatment at 573 K, 773 K, and 948 K are shown in Figs. 8a–8d. Pretreatment conditions are identical to those used during catalytic reaction. These images show that reaction results in major morphological changes. Representative images following each treatment were chosen. Figure 8a shows the SEM of the original silver foil. The long streaks are caused by the polishing of the surface prior to analysis. EDX analysis shows the presence of a significant amount of carbon contamination and traces of sulfur, silica, and chlorine. A sample which was pretreated at 573 K in the reaction mixture is shown in Fig. 8b. The surface appears to be more inhomogeneous. Large, circular islands with a diameter between 50 and 200 nm are formed. Treatment at 773 K leads to the surface shown in Fig. 8c. The surface appears smoother and the islands formed after treatment at 573 K are no longer present. Holes appear at the grain boundaries between silver crystals. Figure 8d shows the surface after treatment at 948 K. The surface exhibits many small crystalline domains similar to those seen in Fig. 8b for the sample treated at 573 K. The holes formed in the sample treated at 948 K are no longer restricted to the crystallite boundaries. They now cover large portions of the previously smooth silver surface.

4. DISCUSSION

Bulk-dissolved oxygen has been often cited in the literature as being the selective partial-oxidation species (3,5,6,8,9,10–13,29,33,34,36). The fact remains, however, that catalysis is a surface process occurring at the surface. O_γ is essentially O_β in that instance when the oxygen segregates into the uppermost atomic layers of silver, where it

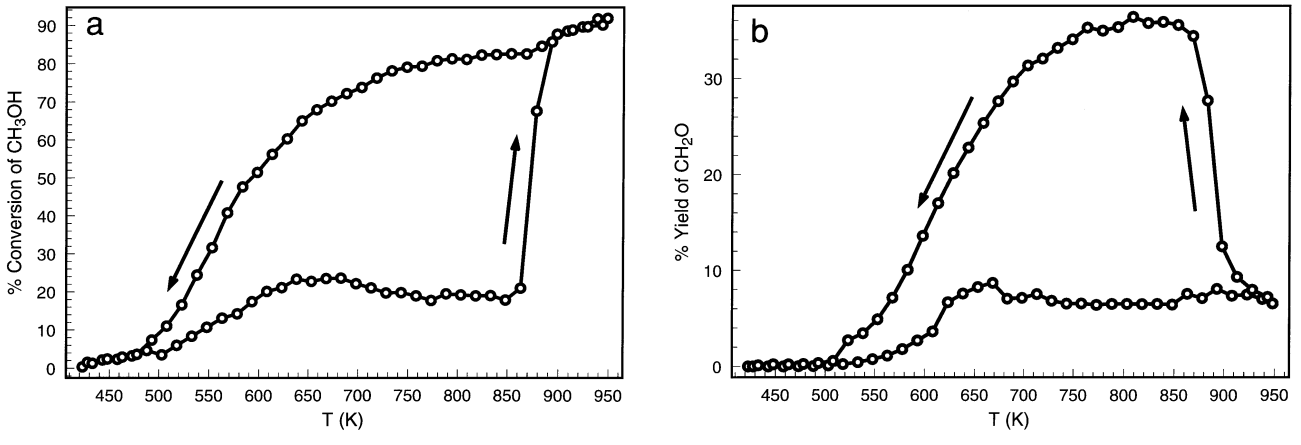

FIG. 5. (a) Percentage conversion of CH_3OH for the cycle (423–948–423 K), 0.5 K/min, 0.06 g Ag + 0.06 g quartz, 4.3 vol% O_2, 7.1 vol% CH_3OH, 88.6 vol% He, S.V. = 1.68×10^5 h^1. (b) Percentage CH_2O yield for the cycle (423–948–423 K), 0.5 K/min, 0.06 g Ag + 0.06 g quartz, 4.3 vol% O_2, 7.1 vol% CH_3OH, 88.6 vol% He, S.V. = 1.68×10^5 h^{-1}.

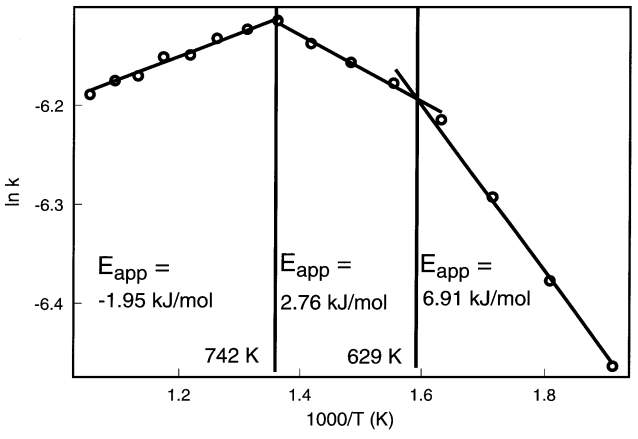

FIG. 6. Arrhenius plot for methanol oxidation over an aged Ag catalyst, 0.3 g aged Ag, (0.2–0.4 mm), 3.5 vol% O_2, 8.8 vol% CH_3OH, 87.7 vol% He, SV = 3.63×10^5 h^{-1}.

may participate in the reaction. The formation of atomically adsorbed O_α, followed by bulk dissolution (O_β) and eventual surface segregation of oxygen, are necessary prerequisites for its formation. O_γ shows an unsaturated thermal desorption peak centered at approximately 1000 K (Fig. 7). The peak is unsaturated because it is impossible to remove all oxygen from silver. One of the underlying principles of thermal desorption spectroscopy assumes that increasing the temperature leads to an increase in the desorption or diffusion rate. This is typically an Arrhenius-type dependence, where the desorption/diffusion rate increases with the exponent of temperature. This assumption requires that solid-state changes do not occur in the material under study which might affect the rate of desorption/diffusion. This is clearly not the case with silver. Silver has a relatively high vapor pressure in vacuum (10). Heating well above the Tamann temperature leads to significant mass transfer from the bulk to the surface, followed by subsequent sublimation and recondensation. Closely packed surface structures are, therefore, formed at the surface, essentially annealing it shut, preventing segregation of oxygen from the bulk to the surface.

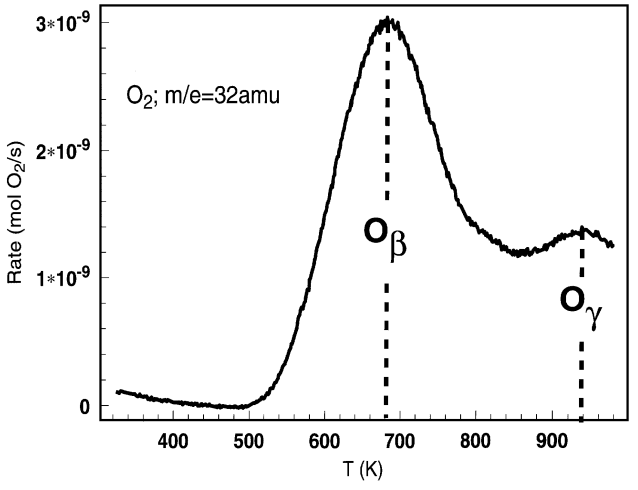

FIG. 7. Oxygen TDS from 1 g electrolytic silver after having been dosed with 100 mbar of O_2 at 973 K for 5 min.

Figure 2 shows that the fresh catalyst is active until approximately 623 K. Comparison with the hysteresis run for this region (Fig. 3) shows that there is no change in the intrinsic activity of the catalyst after reaction under these conditions, hinting that no morphological change of the catalyst is necessary for activation. The SEM image, (Fig. 8b), taken subsequent to this reaction cycle, supports this hypothesis and shows no substantial change in the catalyst surface morphology. The enhancement of the boundaries between the polycrystalline domains seen in this image relative to the fresh sample is caused by the decomposition of Ag_2O ($T_{dec} = 585$ K) which is always present as a contaminant on sample surfaces which have been exposed for longer times to air (18). Oxide formation is enhanced at defect sites resulting in their poorer SEM imaging. Previous work (14,19) has shown that the catalytically active O_α forms readily at these temperatures *via* direct dissociation of molecular oxygen on the surface. The formation of O_α *via* the gas phase shows a strong structure dependence. A number of authors have proposed that defect sites on the silver surface are exceptionally active for the formation of surface-bound atomic oxygen (7,14,26). Figure 2 shows a high yield to complete oxidation products in this temperature range thus providing excellent evidence that O_α is the active species. The absence of holes in Fig.8b, resulting from the reaction of *dissolved* H_2 and O_2 to water (16,21), indicates that the reaction takes place entirely on the surface (22). The catalytically active O_α species is, therefore, formed directly from gas-phase oxygen under these conditions. It forms preferentially on sites of increasing surface-roughness. The sticking coefficient increases as shown: $(111)10^{-7} < (100)10^{-4} < (110)10^{-3} <$ Defects.

To our knowledge, this is the first report of such a hysteresis effect in the literature for this reaction. There are a number of possible explanations why the effect was observed here and nowhere else. Carbon is often reported as a contaminant for studies performed with electrolytic silver (6,7,8,25,29,34). It is possible that previous groups have first treated the sample at elevated temperatures in oxygen in order to burn off carbon impurities. This would lead to a restructuring of the catalyst and an elimination of the hysteresis. Lefferts *et al.* (12) treated their sample in dilute HNO_3 in order to remove impurities. Previous work in our lab has shown that treatment of Ag in NO containing environments leads to the formation of large amounts of $AgNO_3$ and Ag_2O (41). Subsequent decomposition of these samples (thermal or by dissolving in H_2O) reveals a spongy material which has undergone extensive reconstruction.

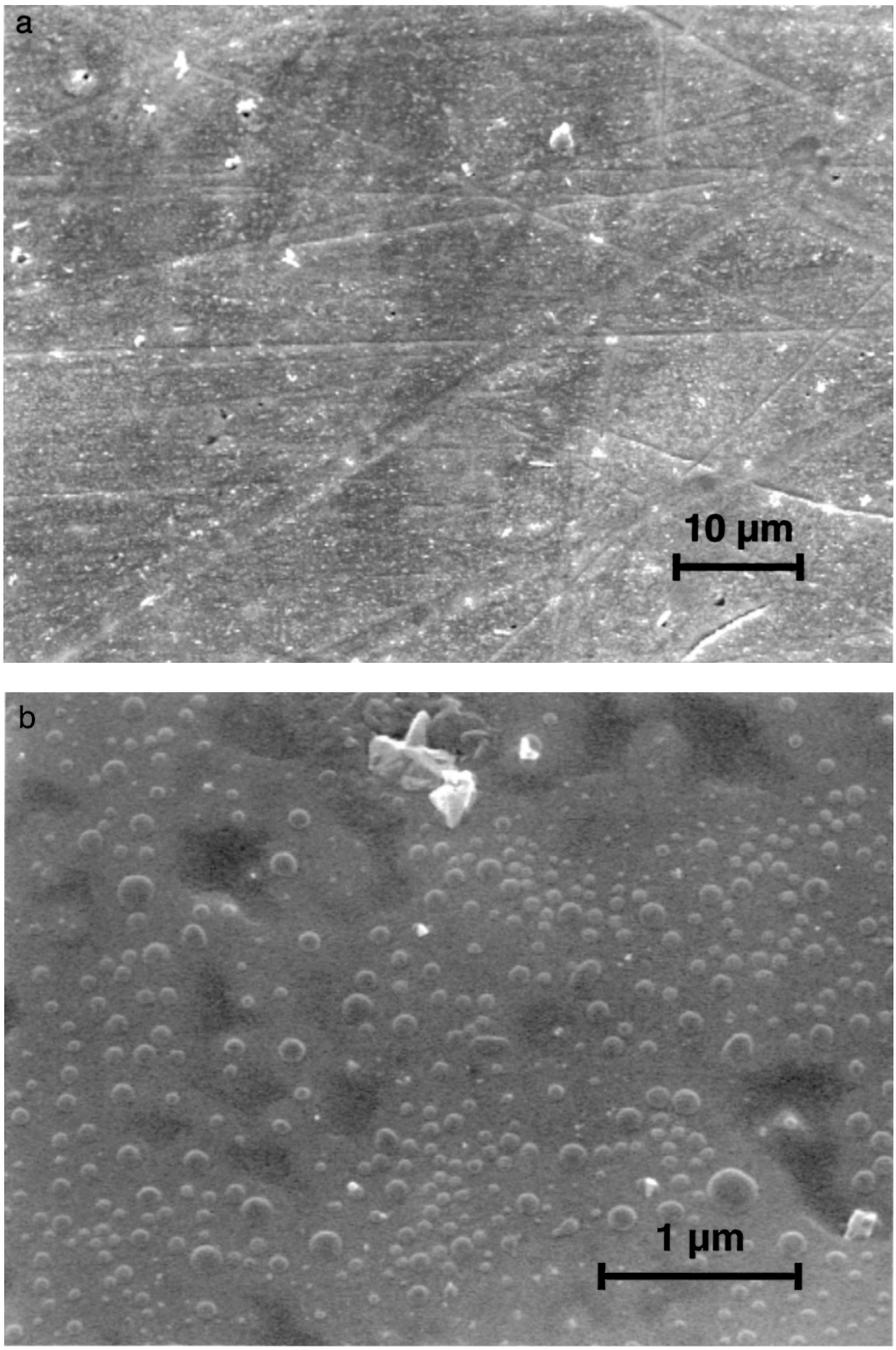

FIG. 8. (a) SEM image of the fresh polycrystalline silver foil. (b) SEM image of the polycrystalline foil after having undergone the reaction cycle (423–573–423 K), 3.5 vol% O_2, 8.8 vol% CH_3OH, 87.7 vol% He. (c) SEM image of the polycrystalline foil after having undergone the reaction cycle (423–773–423 K), 3.5 vol% O_2, 8.8 vol% CH_3OH, 87.7 vol% He. (d) SEM image of the polycrystalline foil after having undergone the reaction cycle (423–948–423 K), 3.5 vol% O_2, 8.8 vol% CH_3OH, 87.7 vol% He.

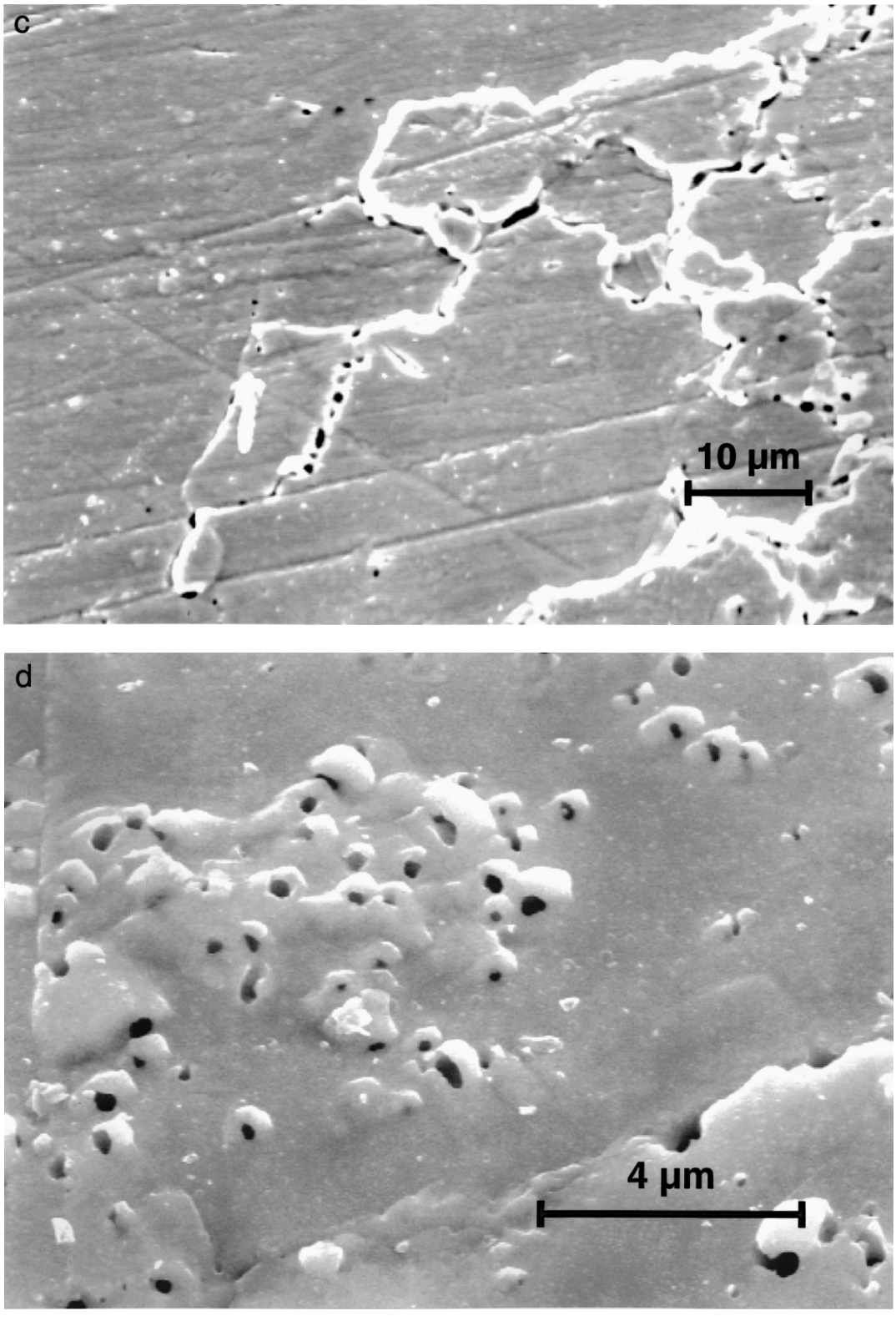

FIG. 8—*Continued*

In another publication by this group (14) it was mentioned that the sample first underwent repeated cycles of oxidation and reduction before testing. This could explain why the deactivation effect was not observed in this study. Finally, any groups which used the same catalyst more than once would have not been able to observe this phenomenon.

The hysteresis run for the cycle (423–773–423 K) (Figs. 4a and 4b) shows that reaction over the fresh sample in this temperature range results in a marked deactivation of the catalyst. Comparison of the conversions seen for the ascending branches of Figs. 4a and 4b with the ascending branches for Figs. 5a and 5b shows the irreversibility of the deactivation occurring during cycle 2. This is evidence that the hysteresis is not due to a temperature bistability of the system but rather to a change in the intrinsic activity of the catalyst itself. Close inspection of the SEM micrographs (Fig. 8c) reveals the origin of this deactivation. Figure 8c shows the surface following this reaction cycle (423–773–423 K). The reaction of O_β with dissolved H_2 to H_2O is evidenced by the holes formed (22). The fact that the holes are located almost entirely at the grain boundaries is evidence for the fact that reaction with bulk oxygen diffusing to and along the defects is taking place in this temperature range. It is also possible that significant mass transport from the crystal grain-boundaries to bulk defects formed during reaction (not visible in SEM) results in the hole formation at the boundaries. The energetically unfavorable location of silver atoms at grain boundaries makes them an excellent source for silver migration ultimately leading to defect healing (23). Ultimately, however, both phenomena originate as a result of hole formation. The formerly polycrystalline surface shows smooth contours indicative of pronounced sintering. The occurrence of this sintering corresponds well to the Tamann temperature which is 750 K for silver ($T_m = 1234$ K). Above this temperature the kinetics of bulk diffusion of the silver are sufficiently fast to result in significant mass transport of silver within the time frame of a typical run. Healing of the defect-rich, polycrystalline surface seen in Fig. 8b *via* sintering explains the pronounced deactivation of the catalyst seen for the hysteresis cycle (423–773–423 K) (Figs. 4a and 4b). The assignment of the deactivation to the inhibition of grain-boundary oxygen diffusion from the silver bulk also stems from the excellent agreement of the TDS desorption temperature for the oxygen species assigned to O_β with the deactivation temperature. This is the peak shown in Fig. 7 centered at approximately 773 K. The asymmetry of this peak hints that it is comprised of a number of desorption signals arising from the diffusion and desorption of several *bulk-species* evolving in the order of increasing diffusion resistance. The temperature regime where catalytic deactivation occurs coincides with this thermal desorption of O_β, indicating that the deactivation is likely due to oxygen diffusion inhibition. It has also been suggested that strongly bound surface oxygen species form preferentially at defects (39,40). These authors suggest that strongly bound oxygen is the active species in this temperature regime. The integral desorption amount for the O_β peak in Fig. 7 corresponds to about 7×10^{-7} mol O_2/g. Approximating the surface area at 0.001 m^2/g (0.4-mm diameter sphere calculation) and assuming a (111) surface structure with an atomic diameter of 2.35 Å yields a value of 2.3×10^{16} atoms/m^2. Assuming 100% coverage, one arrives at a value of about 30 monolyers of oxygen. This represents an absolute worse-case scenario as the surface is not completely (111) oriented and, in reality, exhibits a very low sticking coefficient for oxygen ($<10^{-6}$). Formation of this many monolayers of oxygen at this temperature is impossible and the highest oxygen coverage for silver (111) is actually known to be well below 100% (29,34). The assignment of this peak to a desorbing surface species is therefore impossible. This assignment has also been made by a number of other authors (3,5,6,8). A mechanism in which this subsurface oxygen *dynamically* participates in reaction was, however, never proposed. The fact that a constant feed of O_2 is required for reaction necessarily implies that all active oxygen species are eventually consumed in the course of reaction. The bulk-dissolved oxygen formed under these conditions therefore undergoes equimolar counterdiffusion, where the concentration in the bulk is determined by the balance between rate of O_2 dissolution in Ag and rate of segregation, followed either by O_2 desorption or reaction. Clearly, this cannot be a surface bound atomic oxygen species.

The elimination of the reaction hysteresis is shown in Figs. 5a and 5b (cycle 3). This corresponds well with further structural changes of the silver surface. The SEM image shown in Fig. 8d shows that the hole formation is no longer confined only to grain boundaries, but rather appears to cover large patches of the formerly smooth surface. This likely represents the transition from a system where grain-boundary diffusion and interstitial diffusion through high-indexed planes is the dominant diffusion mechanism to one in which volume diffusion is possible (interstitialcy diffusion). This transition is made possible by the drastic morphological reorientation of the silver surface and bulk after treatment in an oxygen containing atmosphere. It results in the proliferation of holes over the entire surface. The change of silver morphology in various atmospheres has been published elsewhere (6). The catalytic restructuring could only be reversed by heating an aged catalyst (exhibiting no hysteresis) to 973 K in vacuum for 20 min and subsequently testing it again in the flow reactor. Runs made with this sample show a reappearance of the deactivation ($573\ \text{K} < T < 873\ \text{K}$) and a pronounced hysteresis (not shown). Heating in a vacuum is known to result in sublimation and recondensation of silver which results in annealing of the metal surface and bulk with subsequent defect healing. This results in the gradual destruction of

facets, grain boundaries, and holes formed during reaction. The reappearance of the hysteresis after vacuum treatment provides excellent confirmation of the promoting effect of reaction-induced restructuring.

Tests made with catalysts after having undergone high temperature ($T > 923$ K) reaction do not show this hysteresis. Diffusion effects are therefore not directly observable from temperature-conversion plots obtained from tests made with these samples. Subtle changes of the reaction rate are often easier to identify after producing an Arrhenius plot (Fig. 6). The Arrhenius plot has three distinct regions of activity which correlate well with the areas of deactivation seen for the fresh sample (see Fig. 2). This plot shows that diffusion limitations exist for samples which have undergone thermal pretreatment in the reaction atmosphere, although to a much lesser extent than in fresh samples. Lefferts (7) proposed that film-layer diffusion is present under the conditions used here. This explains the exceptionally small apparent activation energies measured in all three temperature regions. The first region corresponds to reaction of surface-bound O_α species formed directly from the gas phase. It extends until the first inflection point seen in the temperature-conversion plot for a fresh silver sample (Fig. 2). The excellent correlation of the TDS O_β desorption signal and the second inflection point in the Arrhenius plot indicates that this is the temperature at which bulk diffusion is activated and reaction with O_γ becomes possible. Because the oxygen conversion is 100%, the CH_3OH conversion is determined by the equilibrium between the oxi-dehydrogenation, direct dehydrogenation, and total oxidation reactions. The inflection, therefore, represents a shift from preferential oxi-dehydrogenation to direct dehydrogenation via reaction with O_γ produced via the O_β segregation. The third region showing extremely low or negative activation energies is attributed to sintering of the reaction-promoting defects formed during reaction at temperatures higher than 773 K. The thermal reordering leading to defect healing occurs at a faster rate than hole production in this temperature regime. The Arrhenius plots, therefore, do not provide any direct kinetic data. The reaction simply occurs to quickly. The plots do show, however, the shift in reaction mechanism occurring when O_β diffusion is activated. They support the hypothesis that the formation of O_γ via bulk-diffusion is a critical step in the reaction mechanism.

Understanding the link between bulk-structural changes and surface reordering is critical to understanding the methanol oxidation reaction mechanism as a whole. It is known that high temperature treatment of silver in oxygen leads to crystallization of the silver bulk exhibiting, primarily, a (331) terminating surface structure (facets) (6). Formation of this structure results in an optimum fit for oxygen diffusion along channels formed perpendicular to the (110) face found in the (331) surface. Facet formation is, however, not observed under the catalytic conditions used here (presence of excess CH_3OH). This is due to the previously mentioned hole formation resulting from dissolution of product hydrogen and subsequent reaction with O_β to form water. Both hydrogen (a major reaction product) and oxygen have high diffusivities in silver ($D_{H2} = 2.82 \times 10^{-3}$ cm^2/s; $D_{O2} = 8.19 \times 10^{-2}$ cm^2/s (24)). Holes function as sites of higher activity (high O_2 sticking coefficient and low diffusion resistance) which eventually results in the increased formation of more holes. The thermal rearrangement of the silver is constantly disrupted by the reaction-induced defect production. This effect has been mentioned by a number of authors in the literature (14,21,39,40). Reaction of silver under methanol oxidation conditions represents an extremely dynamic situation. This is in contrast to facet formation which is observed under conditions where the system is allowed to form equilibrium structures, resulting in an overall decrease in the surface free energy. Hole production as a result of reaction prevents the silver from attaining these equilibrium structures. Reaction remains, therefore, kinetically controlled. This situation is very different from that where the silver is completely facetted. This situation would represent the local thermodynamic energy minimum. Reaction at moderate reaction temperatures (623 K $< T <$ 923 K), occurs primarily with oxygen diffusing along grain boundaries. The fact that hole formation is not restricted to grain boundaries at high temperatures ($T > 923$ K) is clear evidence that volume diffusion (interstitialcy) is also a major reaction pathway. This correlates well with results observed in the literature (24,37) which show that oxygen may diffuse via octahedral hole jumping at lower temperatures ($T <$ 900 K) or via interstitialcy diffusion at elevated temperatures ($T > 900$ K).

Reaction scheme 1 summarizes the proposed mechanism. Gaseous oxygen is dissociatively adsorbed on silver forming O_α. This occurs preferentially on defect sites and crystalline faces of lower coordination. O_α diffuses into the bulk forming O_β. O_α may react at the surface with methanol

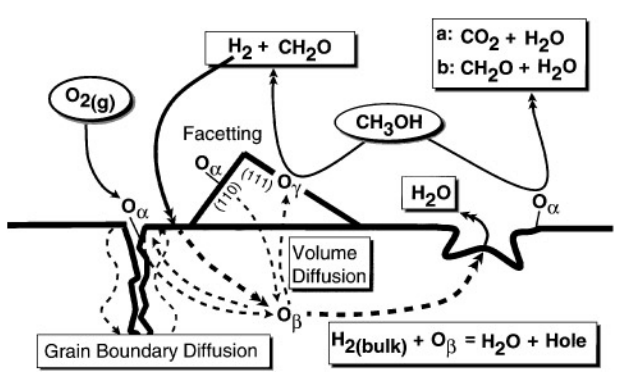

SCHEME 1. Proposed reaction mechansim of silver volume/surface restructuring resulting from reaction with oxygen and methanol.

forming CH_2O and H_2O via oxi-dehydrogenation or may form the complete combustion products CO_2 and H_2O. O_β may diffuse back, forming O_α again, or it will diffuse to a densely packed (111) side of the silver facet. At elevated temperatures, O_β atoms are incorporated *into* the uppermost atomic layers forming O_γ (12). O_γ catalyzes the dehydrogenation of methanol to formaldehyde and hydrogen. Hydrogen formed via this reaction may dissolve into the silver bulk and react with O_β, producing water. This ultimately results in the formation of holes with subsequent desorption of water. The hole formation results in the destruction of the facetted surface. Thermal healing of the silver results in the gradual sintering of holes and defects created during reaction. All of the processes occur simultaneously, resulting in a system which is capable of attaining a dynamic equilibrium which is optimal for catalysis.

This scheme is by no means a complete reaction scheme. There are certainly a number of intermediate products formed during the course of reaction. Furthermore, it is known that gas-phase reactions play a role in the reaction (42). The point of this scheme is to show that reaction with the various species leads, ultimately, to the various products shown.

5. CONCLUSIONS

Treatment of electrolytic silver at elevated temperatures in a reaction mixture consisting of $MeOH/O_2 = 2.5$ results in a restructuring of the catalyst surface and bulk. Reaction with the highly oxidative, surface-bound, atomic-oxygen species O_α dominates at temperatures lower than 623 K. Reaction under these conditions does not result in a change in the catalyst morphology. Severe deactivation of the fresh catalyst in the region $573\ \text{K} < T < 873\ \text{K}$ occurs as a result of the annealing of grain boundaries present in the fresh polycrystalline sample. This sintering hinders the formation of active-surface oxygen via grain-boundary diffusion which is the prevailing mechanism in this temperature regime for fresh silver samples. Treatment of the catalyst at temperatures exceeding 873 K results in a marked morphological change of the catalyst surface structure. Formation of O_γ via volume diffusion is possible under these conditions. This represents, essentially, a system where volume diffusion replaces grain-boundary diffusion as the dominant process for oxygen activation. Hole formation resulting from dehydroxylation of dissolved oxygen and hydrogen results in enhanced defect formation at these higher temperatures. The O_γ oxygen species formed as a result of this high-temperature bulk diffusion process exhibits a less oxidative nature than the surface-bound O_α. The direct dehydrogenation of methanol to formaldehyde is, therefore, enhanced at higher temperatures and the complete oxidation is suppressed. It is shown that morphological changes occur which would otherwise not be found without reaction (pure thermal reordering). The resulting structures provide an optimum for the formation of O_γ via formation of and eventual segregation of O_β to the facetted surface where it may form O_γ. This model is a deviation from the classical idea of a heterogeneously catalyzed surface reaction occurring on a morphologically undefined solid surface. There exists an intimate connection between catalyst morphology and catalytic activity. This interaction strongly influences the steady-state formation of a bulk intermediate which is necessary for the promotion of the desired reaction which occurs at the gas–metal interface.

REFERENCES

1. Ullman, "Ullman's Encyclopedia of Industrial Chemistry," 5th ed., Vol. A11, p. 619. VCH, Weinheim, 1988.
2. Sperber, H., *Chem.-Ing.-Tech.* **41**(17), 962 (1969).
3. Reuss, G., Disteldorf, W., Grundler, O., and Hilt, A., "Formaldehyde," Vol. A11, 619. Verlag Chemie, Weinheim, 1988.
4. Bao, X., Pettinger, B., Ertl, G., and Schlögl, R., *Ber. Bunsenges. Phys. Chem.* **97**(3), 97 (1993).
5. Van Santen, R., and De Groot, C., *J. Catal.* **98**, 530 (1986).
6. Herein, D., Nagy, A., Schubert, H., Weinberg, G., Kitzelmann, E., and Schlögl, R., *Z. Phys. Chem.* **197**, 67 (1996).
7. Schubert, H., Tegtmeyer, U., Herein, D., Bao, X., Muhler, M., and Schlögl, R., *Catal. Lett.* **33**, 305 (1995).
8. Bao, X., Lempfuhl, G., Weinberg, G., Schlögl, R., and Ertl, G., *J. Chem. Soc. Faraday Trans.* **88**(6), 865 (1992).
9. Bao, X., Barth, J. V., Lempfuhl, G., Schaster, R., Uchida, Y., Schlögl, R., and Ertl, G., *Surf. Sci.* **284**, 14 (1993).
10. Bao, X., Muhler, M., Schedel-Niedrig, Th., and Schlögl, R., *Phys. Rev. B* **54**(3), 2249 (1996).
11. Bao, X., Jingfa, D., and Dong, S., *Surf. Sci.* **163**, 444 (1985).
12. Lefferts, L., van Ommen, J. G., and Ross, J. R. H., *Appl. Catal.* **23**, 385 (1986).
13. Bukhtizarov, V. I., Prosvirin, I. P., and Kvon, R. I., *Surf. Sci.* **320**, L47 (1994).
14. Lefferts, L., van Ommen, J. G., and Ross, J. R. H., *Appl Catal.* **31**, 291 (1987).
15. Grant, R. B., and Lambert, R. M., *Surf. Sci.* **146**, 256 (1984).
16. Schubert, H., Tegtmeyer, V., Herein, D., Bao, X., Muhler, M., and Schlögl, R., *Catal. Lett.* **33**, 305 (1995).
17. Herein, D., Werner, H., Schedel-Niedrig, Th., Neisius, Th., Nagy, A., Bernd, S., and Schlögl, R., *in* "Proc. 3rd World Congress on Oxidation Catalysis, Sept. 21–26, 1997" (S. T. Oyama *et al*., Eds.),
18. Bowker, M., *Surf. Sci.* **155**, L276 (1985).
19. Bao, X., Muhler, M., Pettinger, B., Schlögl, R., and Ertl, G., *Catal. Lett.* **22**, 215 (1993).
20. Bao, X., and Deng, J., *J. Catal.* **99**, 391 (1986).
21. Millar, G., Nelson, M., and Uwins, P., *Catal. Lett.* **43**, 97 (1997).
22. Uwins, P., Millar, G., and Nelson, M., *Microsc. Res. Technique* **36**, 382 (1997).
23. Kittel, Ch., "Introduction to Solid-State Physics." Oldenbourg Verlag, Munich, 1988.
24. Eichenauer, W., and Pebeler, A., *Z. Metallkde.* **48**, 373 (1957).
25. Rovida, G., Pratesi, F., Maglietta, M., and Ferroni, E., *Surf. Sci.* **43**, 230 (1974).
26. Frank, E. R., and Hamers, R. J., *J. Catal.* **172**, 406 (1997).
27. Campbell, C. T., *Surf. Sci.* **157**, 43 (1985).
28. Barteau, M. A., and Madix, R. J., *Surf. Sci.* **97**, 101 (1980).
29. Prince, K. C., Paolucci, G., and Bradshaw, A. M., *Surf. Sci.* **175**, 101 (1986).
30. Meima, G. R., Knijf, L. M., van Dillen, A. J., Geus, J. W., Bongaarts, J. E., van Buren, F. R., and Delcour, K., *Catal. Today* **1**, 117 (1987).

31. Rehren, C., Muhler, M., Bao, X., Schlögl, R., and Ertl, G., *Z. Phys. Chem.* **174**, 11 (1991).
32. Haul, R., *Z. Phys. Chem.* **186**, 227 (1994).
33. van Santen, R. A., and Kuipers, H. P. C. E., *Adv. Catal.* **35**, 265 (1987).
34. Backx, C., de Groot, C., and Biloen, P., *J. Catal.* **72**, 364 (1981).
35. Bowker, M., Pudney, P., and Roberts, G., *J. Chem. Soc. Faraday Trans. I* **85**(8), 2635 (1989).
36. Mars, P., and van Krevelen, D. W., *Chem. Eng. Sci. Special Suppl.* **3**, 41 (1954).
37. Outlaw, R. A., Wu, D., Davidson, M. R., and Hoflund, G. B., *J. Vac. Sci. Technol. A* **10**(4), 1497 (1992).
38. Wei, T.-C., and Phillips, J., *Adv. Catal.* **41**, 359 (1995).
39. Lefferts, L., van Ommen, J. G., and Ross, J. R. H., *Appl. Catal.* **34**, 329 (1987).
40. Lefferts, L., van Ommen, J. G., and Ross, J. R. H., *in* Proc. 9th Int. Conf. Catal., Vol. 4, p. 1672. Elsevier Science, Amsterdam, 1988.
41. Zemlyanov, D., Nagy, A., Wild, U., Schedel-Niedrig, Th., and Schlögl, R., The reaction of the NO/O_2 mixture with silver. Part 1. The distribution of compounds with depth, from $AgNO_3$ to metallic silver, *Surf. Sci.*, in press.
42. Aneke, L. F., den Ridder, J. J. J., and van den Berg, P. J., *J. R. Netherlands Chem. Soc.* **100**, 236 (1981).